Fourier, hyperbolic and relativistic heat transfer equations: a comparative analytical study

Juan A. López Molina[1], María J. Rivera[1], Enrique Berjano[2,3]

[1] Applied Mathematics Department, Instituto de Matemática Pura y Aplicada, Universitat Politècnica de València, Valencia, Spain

[2] Biomedical Synergy, Electronic Engineering Department, Universitat Politècnica de València, Valencia, Spain

Abstract

Parabolic heat equation based on Fourier's theory (FHE), and hyperbolic heat equation (HHE), have been used to mathematically model the temperature distributions of biological tissue during thermal ablation. However, both equations have certain theoretical limitations. The FHE assumes an infinite thermal energy propagation speed, while the HHE might possibly be in breach of the second law of thermodynamics. The relativistic heat equation (RHE) is a hyperbolic-like equation, whose theoretical model is based on the theory of relativity and which was designed to overcome these theoretical impediments. In this study the three heat equations for modeling of thermal ablation of biological tissues (FHE, HHE and RHE) were solved analytically and the temperature distributions compared. We found that RHE temperature values were always lower than those of the FHE, while the HHE values were higher than the FHE, except for the early stages of heating and at points away from the electrode. Although both HHE and RHE are mathematically hyperbolic, peaks were only found in the HHE temperature profiles. The three solutions converged for infinite time or infinite distance from the electrode. The percentage differences between the FHE and the other equations were larger for higher values of thermal relaxation time in HHE.

Keywords: Ablation, analytical model, Fourier heat equation, hyperbolic heat equation, radiofrequency heating, relativistic heat conduction, theoretical modeling, thermal ablation, thermal wave.

[3]Address for correspondence: Dr. Enrique Berjano, Electronic Engineering Department, Universitat Politècnica de València, Camino de Vera, 46022 Valencia, Spain. E-mail: eberjano@eln.upv.es

1 Introduction

Energy-based ablative techniques (EBAT) employ certain types of energy (e.g. radiofrequency, microwave, laser, ultrasounds) to destroy or irreversibly alter a target zone of biological tissue. High-temperature EBATs raise temperature tissue over $50°C$ to achieve these results. For instance, radiofrequency (RF) ablation (RFA) is a high-temperature EBAT which uses RF electrical currents to produce coagulative necrosis. It has been broadly used in many procedures such as eliminating cardiac arrhythmias (Wazni *et al* [1] 2011,) and destroying tumors (Salas *et al* [2] 2011). Theoretical modeling has been proposed as a fast and inexpensive approach to developing new EBATs and studying the electrical and thermal phenomena involved in the ablative process (Berjano [3] 2006). To date, most these models have employed the bioheat equation proposed by Pennes [4] 1948 (FHE), in which the heat conduction term is based on Fourier's theory and the heat flux $\overrightarrow{q}\ (\mathbf{x}, t)$ is

$$\overrightarrow{q}\ (\mathbf{x}, t) = -k\nabla T(\mathbf{x}, t) \tag{1}$$

k being thermal conductivity and $T(\mathbf{x}, t)$ temperature. We thus obtain the classical parabolic heat equation:

$$\frac{1}{\alpha}\frac{\partial T}{\partial t}(\mathbf{x}, t) = \Delta T(\mathbf{x}, t) + \frac{1}{k}S(\mathbf{x}, t) \tag{2}$$

where $S(\mathbf{x}, t)$ is the heat source and α is thermal diffusivity. However, FHE assumes an infinite thermal energy propagation speed, which is physically inadmissible. Although this approach might be suitable to model most EBATS, it has been suggested that under certain conditions, such as very short heating times (miliseconds or shorter), a non-Fourier model should be considered (Liu, Chen and Xu [5] (1999), Shih *et al.* [6] (2005), Kaminski [7] (1990), Zhang *et al.* [8] (2006)). About this non-Fourier approach, Morse and Feshbach [9] (1953) proposed a heat equation similar to the telegraph equation, known as Maxwell's equation because it resembles the equation of the propagation of an electromagnetic field, e. g. light, and which is basically a wave equation with a damping term:

$$\frac{1}{C^2}\frac{\partial^2 T}{\partial t^2}(\mathbf{x}, t) + \frac{1}{\alpha}\frac{\partial T}{\partial t}(\mathbf{x}, t) = \Delta T(\mathbf{x}, t) \tag{3}$$

where C is the speed of heat propagation in the medium. Tisza [10] (1938) and Landau [11] (1941) predicted that the speed of heat in a medium can be different from the speed of sound and called it the *second sound* (Ali and Zhang [12] (2005)). Different arguments suggest that the speed of heat is at least one order of magnitude less than the speed of sound. But within non-homogeneous materials, such as biological tissues or in the presence of severe plastic deformation or a high strain rate, the speeds of heat are much lower than in metals and perfect structures. This is because in metals, both heat and sound are propagated by mechanisms, such as lattice vibrations, which are all decelerated by the structural imperfections of biological tissues and non metal materials. Also, some studies have shown that in many cases the values of C and α imply that the first term

of the equation (3) (second order derivative) does not have to be necessarily negligible with respect to the second term (first order derivative) (Mitra et al. [13] (1995), Ali and Zhang [12] (2005)). With the same purpose, Cattaneo [14] (1958) and Vernotte [15] (1958) proposed a modification of Fourier's linear flux as follows

$$\overrightarrow{q}\ (\mathbf{x},t)+\tau\frac{\partial\ \overrightarrow{q}}{\partial t}(\mathbf{x},t)=-k\nabla T(\mathbf{x},t) \tag{4}$$

considering a non zero thermal relaxation time τ of the heat conduction for the medium, that is, there is a response time lag between the heat flux vector and the temperature gradient. Tzou [16] (1992) provided a macroscopic formulation of the problem considering that due to this delay the temperature gradient at time t results in a heat flux at a later time $t+\tau$

$$\overrightarrow{q}\ (\mathbf{x},t+\tau)=-k\nabla T(\mathbf{x},t) \tag{5}$$

obtaining equation (4) after substituting $\overrightarrow{q}\ (\mathbf{x},t+\tau)$ for its first order Taylor expansion. Then we obtain the corresponding modification of the heat flux law by direct integration:

$$\overrightarrow{q}\ (\mathbf{x},t)=-\frac{k}{\tau}\,e^{-\frac{t}{\tau}}\int_0^t e^{\frac{v}{\tau}}\nabla T(\mathbf{x},v)\,dv \tag{6}$$

With this new approach, the result is the hyperbolic heat equation (HHE) (Özişik and Tzou [17] 1994):

$$\frac{\tau}{\alpha}\frac{\partial^2 T}{\partial t^2}(\mathbf{x},t)+\frac{1}{\alpha}\frac{\partial T}{\partial t}(\mathbf{x},t)=\Delta T(\mathbf{x},t)+\frac{1}{k}\left(S(\mathbf{x},t)+\tau\ \frac{\partial S}{\partial t}(\mathbf{x},t)\right) \tag{7}$$

In the absence of heat sources ($S(\mathbf{x},t)=0$), this equation is identical to the Maxwell equation taking $C^2=\frac{\alpha}{\tau}$.

However, the formulation of HHE has a problem. There are differences between FHE and HHE from a thermodynamic point of view. When they are analyzed within the framework of the traditional irreversible thermodynamics, which is based on the assumption of local equilibrium, FHE yields an expression for the entropy production rate which is always non-negative. In contrast, Eq. (4) yields an expression for the entropy production rate which, under certain circumstances (see Barletta and Zanchini [18] (1997)), can assume negative values, which contradicts the second law of thermodynamics. It should be emphasized that a generally accepted theory of irreversible thermodynamics, in which local equilibrium is released, is not yet available. Of course, this does not necessarily mean that HHE violates a non-equilibrium second law, if such a law can be established, but it cannot be ruled out. Moreover a non-equilibrium equation that yields an expression of the entropy production rate which is non-negative is likely to satisfy a more general non-equilibrium second law.

To overcome the problems involved in FHE and HHE, Ali and Zhang [12] (2005) proposed a theoretical model based on a weak interpretation of the theory of relativity. In this setting, relativistic does not mean "concerned with objects moving at speeds comparable

to the speed of light", but "concerning objects that move or propagate at speed comparable with a limiting speed characteristic of the field or medium involved, denoted by C". For example, the speed of the photon in electromagnetism, speed of light in a vacuum, speed of the graviton in cosmology, speed of sound in wave propagation in fluids, and the limiting speed of heat in heat conduction problems in gas and solid media. Consequently, this theory ensures a finite thermal energy propagation speed.

Ali and Zhang's relativistic model adds the time coordinate t to the three Euclidean coordinates (x, y, z). In relativistic physics it is usual to work in a four-dimensional pseudo-Euclidean space-time (ζ, x, y, z), where ζ is the so called "spacelike-time", has a length dimension and moreover, $\zeta = i\ C\ t$, where i is the imaginary unit constant and C is a constant with a velocity dimension, ensuring in this way that ζ remains orthogonal to the other three spatial dimensions, with respect to Minkowski metrics

$$ds^2 = dx^2 + dy^2 + dz^2 - C^2 dt^2 \tag{8}$$

which remains invariant in all inertial frames of reference. Then the four-dimensional gradient vector will be

$$\Box := \left(\frac{\partial}{\partial\zeta}, \frac{\partial}{\partial x}, \frac{\partial}{\partial y}, \frac{\partial}{\partial z}\right) = \left(-\frac{i}{C}\ \frac{\partial}{\partial t}, \frac{\partial}{\partial x}, \frac{\partial}{\partial y}, \frac{\partial}{\partial z}\right)$$

and the four-dimensional Laplacian (or d'Alembertian $\Box^2$) is

$$\Box^2 := \frac{\partial^2}{\partial\zeta^2} + \frac{\partial^2}{\partial x^2} + \frac{\partial^2}{\partial y^2} + \frac{\partial^2}{\partial z^2} = \frac{-1}{C^2}\ \frac{\partial^2}{\partial t^2} + \frac{\partial^2}{\partial x^2} + \frac{\partial^2}{\partial y^2} + \frac{\partial^2}{\partial z^2}$$

In this setting, Fourier's flux law takes the form

$$\overrightarrow{q}\ (\mathbf{x}, t) = -k\ \Box T(\mathbf{x}, t) \tag{9}$$

and, after the standard arguments, Ali and Zhang's relativistic heat equation turns out to be

$$\frac{\partial T}{\partial t}(\mathbf{x}, t) + \frac{\alpha}{C^2}\frac{\partial^2 T}{\partial t^2}(\mathbf{x}, t) = \alpha\left(\frac{\partial^2 T}{\partial x^2}(\mathbf{x}, t) + \frac{\partial^2 T}{\partial y^2}(\mathbf{x}, t) + \frac{\partial^2 T}{\partial z^2}(\mathbf{x}, t)\right) + \frac{\alpha}{k}\ S(\mathbf{x}, t) \tag{10}$$

where C (assumed to be constant) is the speed of heat propagation in the medium.

This relativistic heat equation (RHE) in a four-dimensional space-time turns out to be identical to the Maxwell equation, is derived without any microscopic or material-specific considerations, and overcomes thermodynamic contradictions, as has been shown by Ali and Zhang [12] (2005). Moreover, except for the terms involving the heat source $S(\mathbf{x}, t)$, RHE (10) is mathematically identical to HHE (7), but the HHE heat flux is based on (4) and the RHE heat flux on (7). That is why RHE has good thermodynamic behaviour.

Since this difference in the flux computations involves different mathematical expressions in the boundary conditions of RHE and HHE, the corresponding solutions could also be different. It is necessary to emphasize that Ali and Zhang [12] (2005) only proposed

the mathematical formulation of the relativistic problem and they did not solve it in any specific case. Our objective was therefore to solve the relativistic problem for the concrete case of thermal ablation of biological tissues (including an internal heat source) in order to compare the temperature distributions in the tissue computed theoretically from the three heat equations (Fourier, hyperbolic, and relativistic). This case was considered since experimental data have suggested that the thermal relaxation time in biological tissues could be significant ([13] (1995)). The analytical solutions for the HHE and FHE were previously obtained (López Molina *et al* [19] 2008). In this study we first obtained the analytical solution to RHE for RFA, and then compared the corresponding solutions in terms of computer temperature distributions.

2 Methods

2.1 Description of the model for RHE

In order to achieve an analytical solution, we considered a model based on a spherical electrode of radius r_0 completely embedded and in close contact with the biological tissue, which has an infinite dimension. As a result, the model has a radial symmetry, and a one-dimensional approach is possible. We can then write $T(r,t)$ instead of $T(\mathbf{x},t)$. For thermal ablations based on RFA, the source term in the tissue is the Joule heat produced per unit volume of tissue, $S(r)$, which can be expressed as (Erez and Shitzer [21] 1980):

$$S(r) = \frac{P\, r_0}{4\, \pi\, r^4}; \quad r \geq r_0 \tag{11}$$

where P is the total applied power (W). In our case we use spherical coordinates and all the involved functions are independent of the spherical angles. The resulting RHE is

$$-\alpha \left(\frac{\partial^2 T}{\partial r^2}(r,t) + \frac{2}{r}\frac{\partial T}{\partial r}(r,t) \right) + \frac{\partial T}{\partial t}(r,t) + \frac{\alpha}{C^2}\frac{\partial^2 T}{\partial t^2} = \frac{P\, r_0}{4\, \pi\, r^4} \tag{12}$$

The initial and boundary conditions are

$$T(r,0) = T_0, \qquad \frac{\partial T}{\partial t}(r,0) = 0 \qquad \forall r > 0$$

$$\lim_{r\to\infty} T(r,t) = T_0 \qquad \forall t > 0$$

where T_0 is the initial temperature. To write the boundary condition in $r = r_0$ we shall adopt a simplification used in Erez and Shitzer [21] (1980), assuming the thermal conductivity of the electrode to be much greater than that of the tissue (i.e. assuming that the boundary condition at the interface between electrode and tissue is mainly governed by the thermal inertia of the electrode). At every time t the modulus of the heat flux along the surface electrode by unit time is

$$4\, \pi\, k\, r_0^2 \sqrt{\frac{-1}{C^2}\left(\frac{\partial T}{\partial t}(r_0,t)\right)^2 + \left(\frac{\partial T}{\partial r}(r_0,t)\right)^2}$$

which is inverted to produce a heat increment in the mass electrode equal to

$$\nu_0\, c_0\, \frac{4\,\pi r_0^3}{3} \frac{\partial T}{\partial t}(r_0, t)$$

where ν_0 and c_0 are the density and specific heat of the active electrode, respectively. Then the boundary condition in $r = r_0$ must be

$$4\,\pi\,k\,r_0^2 \sqrt{\frac{-1}{C^2}\left(\frac{\partial T}{\partial t}(r_0,t)\right)^2 + \left(\frac{\partial T}{\partial r}(r_0,t)\right)^2} = \nu_0\, c_0\, \frac{4\,\pi r_0^3}{3} \frac{\partial T}{\partial t}(r_0,t) \tag{13}$$

or equivalently

$$A\, \frac{\partial T}{\partial t}(r_0,t) = \frac{\partial T}{\partial r}(r_0,t) \tag{14}$$

where $A := \frac{1}{k}\sqrt{\nu_0^2\, c_0^2\, \frac{r_0^2}{9} + \frac{k^2}{C^2}}$.

2.2 Comparison of models

Once the RHE analytical solution was obtained, we compared the three models (FHE, HHE, RHE) by plotting temperature distributions and evolution with Mathematica 6.0 (Wolfram Research Inc. Champaign, IL, USA). Even though some results were plotted using dimensionless variables, we had to consider specific values for some parameters of the model: electrode radius $r_0 = 1.5$ mm, constant power $P = 1$ W, initial temperature $T_0 = 37$°C, tissue density $\nu = 1200$ kg m^{-3}, tissue specific heat $c = 3200$ J kg^{-1} K^{-1}, tissue thermal conductivity $k = 0.7$ W m^{-1}K^{-1}, electrode density $\nu_0 = 21\,500$ kg m^{-3} and electrode specific heat $c_0 = 132$ J kg^{-1}K^{-1}. These values have been used in previous modeling studies (López Molina *et al.* [19] 2008). The dimensionless thermal relaxation time of the biological tissue for HHE was $\lambda = 1.2963$ which is equivalent to $\tau = 16$ s. This value was initially suggested by Mitra *et al.* [13] (1995) in processed meat. In RHE appears a parameter C which depends on the medium properties. To compare with the HHE, we chose C in such a way that $C^2 = \frac{\alpha}{\tau}$ so that the coefficients of the governing equation would be the same in both models, even though this procedure did not ensure the exact replication of the physical reality. It is noteworthy that with the values of the parameters considered in this study, C takes a theoretical value as small as $C = 9.07 \times 10^{-5}$m/s, in good agreement with the qualitative indications given in Ali and Zhang [12] (2005). To date, there are no experimental data about the value of C.

3 Results

3.1 Relativistic heat model

To solve analytically the RHE for a spherical electrode, we chose dimensionless variables

$$\rho := \frac{r}{r_0}, \quad \xi := \frac{\alpha\, t}{r_0^2}, \quad \lambda := \left(\frac{\alpha}{r_0\, C}\right)^2, \qquad V(\rho,\xi) := \frac{4\,\pi\,k\,r_0}{P}\left(T\left(r_0\,\rho, \frac{r_0^2\,\xi}{\alpha}\right) - T_0\right)$$

and defined $B := \frac{A\,\alpha}{r_0}$.

The dimensionless problem was to find $V(\rho,\xi)$ such that

$$-\left(\frac{\partial^2 V}{\partial\,\rho^2}+\frac{2}{\rho}\frac{\partial V}{\partial\,\rho}\right)+\frac{\partial V}{\partial\,\xi}+\lambda\,\frac{\partial^2 V}{\partial\,\xi^2}=\frac{1}{\rho^4} \tag{15}$$

$$V(\rho,0)=0,\quad \frac{\partial V}{\partial\xi}(\rho,0)=0\qquad \forall\rho>1$$

$$\lim_{\rho\to\infty} V(\rho,\xi)=0\quad \forall\,\xi>0$$

$$B\,\frac{\partial V}{\partial\xi}(1,\xi)=\frac{\partial V}{\partial\rho}(1,\xi)\quad \forall\,\xi>0$$

Taking Laplace transforms $\mathfrak{L}(\rho,s) := \mathfrak{L}_\xi[V(\rho,\xi)](\rho,s)$ with respect to ξ, we obtained

$$-\left(\frac{\partial^2 \mathfrak{L}}{\partial\,\rho^2}+\frac{2}{\rho}\frac{\partial \mathfrak{L}}{\partial\,\rho}\right)+\left(s+\lambda\,s^2\right)=\frac{1}{\rho^4\,s} \tag{16}$$

$$\lim_{\rho\to\infty}\mathfrak{L}(\rho,s)=0 \tag{17}$$

$$B\,s\,\mathfrak{L}(1,s)=\frac{\partial \mathfrak{L}}{\partial\,\rho}(1,s) \tag{18}$$

Using the new function $z(\rho,s) := \rho\,\mathfrak{L}(\rho,s)$ and the variation of parameters method we obtained the general solution of (16)

$$\mathfrak{L}(\rho,s)=-\frac{e^{\sqrt{s+\lambda\,s^2}\,\rho}}{2\,\rho\,\sqrt{s+\lambda\,s^2}}\left(\frac{1}{s}\int_1^\rho \frac{e^{-\sqrt{s+\lambda\,s^2}\,u}}{u^3}\,du+M_1(s)\right)$$

$$+\frac{e^{-\sqrt{s+\lambda\,s^2}\,\rho}}{2\,\rho\,\sqrt{s+\lambda\,s^2}}\left(\frac{1}{s}\int_1^\rho \frac{e^{\sqrt{s+\lambda\,s^2}\,u}}{u^3}\,du+M_2(s)\right) \tag{19}$$

where $M_1(s)$ and $M_2(s)$ are functions to be determined in order to verify the boundary conditions.

To satisfy (17) we needed to choose

$$M_1(s)=\int_1^\infty \frac{e^{-\sqrt{s+\lambda\,s^2}\,u}}{2\,s\,\sqrt{s+\lambda\,s^2}}\,\frac{du}{u^3}$$

and hence

$$M_2(s)=\frac{\sqrt{s+\lambda\,s^2}-(1+B\,s)}{\sqrt{s+\lambda\,s^2}+(1+B\,s)}\int_1^\infty \frac{e^{-\sqrt{s+\lambda\,s^2}\,(u-2)}}{2\,s\,\sqrt{s+\lambda\,s^2}}\,\frac{du}{u^3}.$$

Then we obtained

$$\mathfrak{L}(\rho,s)=\frac{1}{2\,\rho}\int_\rho^\infty \frac{e^{-\sqrt{s+\lambda\,s^2}\,(u-\rho)}}{s\,\sqrt{s+\lambda\,s^2}}\,\frac{du}{u^3}+\frac{1}{2\,\rho}\int_1^\rho \frac{e^{-\sqrt{s+\lambda\,s^2}\,(\rho-u)}}{s\,\sqrt{s+\lambda\,s^2}}\,\frac{du}{u^3}$$

$$+\frac{1}{2\,\rho}\int_1^\infty \frac{\sqrt{s+\lambda\,s^2}-(1+B\,s)}{\sqrt{s+\lambda\,s^2}+(1+B\,s)}\;\frac{e^{-\sqrt{s+\lambda\,s^2}\,(\rho+u-2)}}{s\,\sqrt{s+\lambda\,s^2}}\;\frac{du}{u^3} \tag{20}$$

and hence

$$V(\rho,s)=\frac{1}{2\,\rho}\big(\mathfrak{L}^{-1}\big[F_1\big]+\mathfrak{L}^{-1}\big[F_2\big]+\mathfrak{L}^{-1}\big[F_3\big]\big) \tag{21}$$

where

$$F_1=\int_\rho^\infty \frac{e^{-\sqrt{s+\lambda\,s^2}\,(u-\rho)}}{s\,\sqrt{s+\lambda\,s^2}}\;\frac{du}{u^3},$$

$$F_2=\int_1^\rho \frac{e^{-\sqrt{s+\lambda\,s^2}\,(\rho-u)}}{s\,\sqrt{s+\lambda\,s^2}}\;\frac{du}{u^3}$$

and

$$F_3=\int_1^\infty \frac{\sqrt{s+\lambda\,s^2}-(1+B\,s)}{\sqrt{s+\lambda\,s^2}+(1+B\,s)}\;\frac{e^{-\sqrt{s+\lambda\,s^2}\,(\rho+u-2)}}{s\,\sqrt{s+\lambda\,s^2}}\;\frac{du}{u^3}=$$

$$\int_1^\infty \frac{e^{-\sqrt{s+\lambda\,s^2}\,(\rho+u-2)}}{s\,\sqrt{s+\lambda\,s^2}}\left(1-\frac{2\,(1+B\,s)}{\sqrt{s+\lambda\,s^2}+(1+B\,s)}\right)\;\frac{du}{u^3}.$$

The computation of the inverse Laplace transforms $\mathfrak{L}^{-1}[F_1],\mathfrak{L}^{-1}[F_2]$ and $\mathfrak{L}^{-1}[F_3]$ is found in the Appendix. According to (21) we obtained

$$V(\rho,\xi)=\frac{1}{2\,\rho}\left(\int_\rho^{\rho+\frac{\xi}{\sqrt{\lambda}}}\left(\int_{(u-\rho)\sqrt{\lambda}}^{\xi}\frac{e^{-\frac{v}{2\lambda}}}{\sqrt{\lambda}}I_0\left(\frac{1}{2\lambda}\sqrt{v^2-\lambda(u-\rho)^2}\right)\,dv\right)\;\frac{du}{u^3}\right.$$

$$+\overline{H}\left(1-\rho+\frac{\xi}{\sqrt{\lambda}}\right)\int_1^\rho\left(\int_{(\rho-u)\sqrt{\lambda}}^{\xi}\frac{e^{-\frac{v}{2\lambda}}}{\sqrt{\lambda}}I_0\left(\frac{1}{2\lambda}\sqrt{v^2-\lambda(\rho-u)^2}\right)\,dv\right)\;\frac{du}{u^3}$$

$$+H\left(\rho-\frac{\xi}{\sqrt{\lambda}}-1\right)\int_{\rho-\frac{\xi}{\sqrt{\lambda}}}^\rho\left(\int_{(\rho-u)\sqrt{\lambda}}^{\xi}\frac{e^{-\frac{v}{2\lambda}}}{\sqrt{\lambda}}I_0\big(\frac{1}{2\lambda}\sqrt{v^2-\lambda(\rho-u)^2}\big)\,dv\right)\;\frac{du}{u^3}$$

$$\left.+H\left(\frac{\xi}{\sqrt{\lambda}}-\rho+1\right)\int_1^{\frac{\xi}{\sqrt{\lambda}}-\rho+2}\left(\int_{\sqrt{\lambda}(u+\rho-2)}^{\xi}G_1(\rho,w)G_2(\xi-w)\,dw\right)\;\frac{du}{u^3}\right) \tag{22}$$

where $H(x)$ is the Heaviside function, $\overline{H}(x)=0$ if $x\le 0$ and $\overline{H}(x)=1$ if $x>0$,

$$G_1(\rho,\xi)=\frac{e^{-\frac{\xi}{2\lambda}}}{\sqrt{\lambda}}\;I_0\left(\frac{1}{2\lambda}\sqrt{\xi^2-\lambda(u+\rho-2)^2}\right) \tag{23}$$

and

$$G_2(\xi)=-1+\left(B+\frac{1}{s_1}\right)\frac{4\,e^{\xi\,s_1}(1+B\,s_1)}{1-2\,B+(2\,\lambda-2\,B^2)\,s_1}+$$

$$\frac{2}{\pi}\int_0^{\frac{1}{\lambda}}\left(B-\frac{1}{s}\right)\frac{\sqrt{s-\lambda s^2}\,e^{-s\,\xi}}{\big(-1-(1-2\,B)\,s+(\lambda-B^2)\,s^2\big)}\,ds \tag{24}$$

3.2 Hyperbolic and Fourier heat models

The dimensionless problem of the FHE is to find $V_F(\rho,\xi)$ such that

$$-\left(\frac{\partial^2 V_F}{\partial\rho^2}+\frac{2}{\rho}\frac{\partial V_F}{\partial\rho}\right)+\frac{\partial V_F}{\partial\xi}=\frac{1}{\rho^4} \tag{25}$$

$$V_F(\rho,0)=0,\quad \frac{\partial V_F}{\partial\xi}(\rho,0)=0\quad\forall\,\rho>1$$

$$\lim_{\rho\to\infty}V_F(\rho,\xi)=0\quad\forall\,\xi>0$$

$$\frac{m}{3}\frac{\partial V_F}{\partial\xi}(1,\xi)=\frac{\partial V_F}{\partial\rho}(1,\xi)\quad\forall\,\xi>0$$

where $m=\frac{\nu_0\,c_0}{\nu\,c}$ is the dimensionless electrode thermal inertia. The solution of this problem was previously presented in López Molina *et al* [19] (2008), and we can express it as follows:

$$V_F(\rho,\xi)=\frac{1}{2\rho}\int_1^\infty\Big(\int_0^\xi\frac{e^{-\frac{(\rho-u)^2}{4x}}}{\sqrt{\pi\,x}}\,dx\Big)\frac{du}{u^3}+$$

$$\frac{1}{2\rho}\int_1^\infty\left(\int_0^\xi\frac{e^{-\frac{(u+\rho-2)^2}{4v}}}{\sqrt{\pi\,v}}\left(-1+\frac{2}{\pi}\int_0^\infty\Big(\frac{m}{3}-\frac{1}{s}\Big)\frac{\sqrt{s}\,e^{-s(\xi-v)}}{-1-(1-\frac{2m}{3})s-\frac{m^2}{9}s^2}\,ds\right)dv\right)\frac{du}{u^3} \tag{26}$$

Likewise, the dimensionless problem for the HHE is to find $V_H(\rho,\xi)$ such that

$$-\left(\frac{\partial^2 V_H}{\partial\rho^2}+\frac{2}{\rho}\frac{\partial V_H}{\partial\rho}\right)+\frac{\partial V_H}{\partial\xi}+\lambda\,\frac{\partial^2 V_H}{\partial\xi^2}=\frac{1}{\rho^4}\big(H(\xi)+\lambda\delta(\xi)\big) \tag{27}$$

$$V_H(\rho,0)=0,\quad \frac{\partial V_H}{\partial\xi}(\rho,0)=0\quad\forall\,\rho>1$$

$$\lim_{\rho\to\infty}V_H(\rho,\xi)=0\quad\forall\,\xi>0$$

$$\frac{\partial V_H}{\partial\xi}(1,\xi)+\lambda\frac{\partial^2 V_H}{\partial\xi^2}(1,\xi)=\frac{3}{m}\,\frac{\partial V_H}{\partial\rho}(1,\xi)\quad\forall\,\xi>0$$

where $H(\xi)$ is the Heaviside function, $\delta(\xi)$ is the Dirac's delta function, $\lambda=\frac{\alpha\,\tau}{r_0^2}$ and m is the dimensionless electrode thermal inertia as above. The analytical solution of HHE was also obtained in López Molina *et al* [19] (2008), where was already demonstrated that $\lim_{\lambda\to0}V_H(\rho,\xi)=V_F(\rho,\xi)$; i.e. the FHE solution is equal to the HHE solution in the case of zero thermal relaxation time.

3.3 The FHE solution as a limit to the RHE solution

It was therefore important to study the behavior of the solution versus the values of C. In this respect, we will now see that $\lim_{C\to\infty} V(\rho,\xi) = V_F(\rho,\xi)$, i. e. the relativistic solution is continuous with respect to C and the FHE solution is the limit to the RHE solution. This is equivalent so saying that $\lim_{\lambda\to 0} V(\rho,\xi) = V_F(\rho,\xi)$.

To prove this fact, we use the asymptotic expansion

$$I_0(x) = \frac{e^x}{\sqrt{2\,\pi\,x}}\left(1 + \frac{1}{8\,x} + \frac{1^2\,3^2}{2!\,(8\,x)^2} + ...\right)$$

given in Watson [23] (1995). Then we have

$$\lim_{\lambda\to 0} \frac{e^{-\frac{v}{2\,\lambda}} I_0\left(\frac{1}{2\,\lambda}\sqrt{v^2-\lambda(u-\rho)^2}\right)}{\sqrt{\lambda}} = \lim_{\lambda\to 0} \frac{e^{\frac{\sqrt{v^2-\lambda(u-v)^2}-v}{2\,\lambda}}}{\sqrt{\lambda}\sqrt{2\,\pi\,\frac{\sqrt{v^2-\lambda(u-\rho)^2}}{2\,\lambda}}} = \frac{1}{\sqrt{\pi\,v}}\,e^{-\frac{(u-\rho)^2}{4\,v}}$$

Analogously we find

$$\lim_{\lambda\to 0} \frac{e^{-\frac{v}{2\,\lambda}} I_0\left(\frac{1}{2\,\lambda}\sqrt{v^2-\lambda(u+\rho-2)^2}\right)}{\sqrt{\lambda}} = \frac{1}{\sqrt{\pi\,v}}\,e^{-\frac{(u+\rho-2)^2}{4\,v}}$$

Then it follows that

$$\lim_{\lambda\to 0} \mathfrak{L}^{-1}\big[F_1\big](\rho,\xi) =$$

$$\lim_{\lambda\to 0} \frac{1}{\sqrt{\lambda}} \int_{\rho}^{\rho+\frac{\xi}{\sqrt{\lambda}}} \left(\int_{(u-\rho)\sqrt{\lambda}}^{\xi} e^{-\frac{v}{2\,\lambda}} I_0\left(\frac{1}{2\,\lambda}\sqrt{v^2-\lambda(u-\rho)^2}\right)\,dv \right) \frac{du}{u^3} =$$

$$\int_{\rho}^{\infty} \left(\int_0^{\xi} \frac{e^{-\frac{(u-\rho)^2}{4v}}}{\sqrt{\pi\,v}}\,dv \right) \frac{du}{u^3}$$

In the same way

$$\lim_{\lambda\to 0} \mathfrak{L}^{-1}\big[F_2\big](\rho,\xi) = \int_1^{\rho} \left(\int_0^{\xi} \frac{e^{-\frac{(u-\rho)^2}{4v}}}{\sqrt{\pi\,v}}\,dv \right) \frac{du}{u^3} \tag{28}$$

Then it follows that

$$\lim_{\lambda\to 0} \big(\mathfrak{L}^{-1}\big[F_1\big](\rho,\xi) + \mathfrak{L}^{-1}\big[F_2\big](\rho,\xi) \big) = \int_1^{\infty} \left(\int_0^{\xi} \frac{e^{-\frac{(u-\rho)^2}{4v}}}{\sqrt{\pi\,v}}\,dv \right) \frac{du}{u^3} \tag{29}$$

With respect to $\lim_{\lambda\to 0} \mathfrak{L}^{-1}\big[F_3\big](\rho,\xi)$ we recall that for small values of λ there are no poles of the function

$$\frac{1}{s(\sqrt{s+\lambda s^2} + (1 + B\,s))}$$

with negative real part. Moreover, it is easy to see that $B = \sqrt{\frac{m^2}{9} + \lambda}$, hence $\lim_{\lambda \to 0} B = \frac{m}{3}$. Then

$$\lim_{\lambda \to 0} \mathfrak{L}^{-1}\big[F_3\big](\rho, \xi) =$$

$$\int_1^\infty \left(\int_0^\xi \frac{e^{-\frac{(u+\rho-2)^2}{4\,v}}}{\sqrt{\pi\, v}} \left(-1 + \frac{2}{\pi} \int_0^\infty (\frac{m}{3} - \frac{1}{s}) \frac{\sqrt{s}\, e^{-s(\xi - v)}}{-1 - (1 - \frac{2m}{3})s - \frac{m^2}{9} s^2}\, ds \right) dv \right) \frac{du}{u^3} \quad (30)$$

In consequence $\lim_{C \to \infty} V(\rho, \xi) = V_F(\rho, \xi)$.

3.4 Comparison of the solutions

Figure 1 shows the dimensionless temperature profiles during RF heating of biological tissue along the radial axis for two different dimensionless times ($\xi = 1$ and $\xi = 7$) obtained from the FHE, HHE and RHE equations. Figure 2 shows the dimensionless temperature evolution during RF heating of biological tissue at two dimensionless locations: $\rho = 1.5$ and $\rho = 2.5$. The most important result was the evolution of the values obtained for each solution: RHE temperature values were always lower than those of the FHE, while HHE values were higher than the FHE except in the early stages of heating and at points away from the electrode (see for instance temperature at $\xi = 1$ for $\rho > 2.2$ in Fig. 1, or temperature at $\rho = 2.5$ for $\xi < 1.5$ in Fig. 2). The three solutions converged for infinite time or infinite distance from the heat source. The RHE solution converged towards FHE quicker than the HHE.

Figure 2 shows the peaks in the temperature profile obtained from the HHE, which were due to the hyperbolic nature of (27), which includes an essential part of the irregularities of the source term in its solutions (i.e. presence of the Heaviside and Dirac distributions). Such peaks are detected too in numerical treatment of these problems, but they are difficult to represent in numerical plots where they appear smoothed, and this fact is reported in [20] (2007). In contrast, although (15) is also hyperbolic, the source term is much more regular (without Heaviside and Dirac distributions), and hence the solution to the RHE equation does not have these peaks (see Fig. 2).

Figure 3 shows the temperature profiles and temperature evolution in dimensional values as an indication of the absolute differences between the three equations. These profiles were obtained for a thermal relaxation time of 16 s in the case of HHE and a value for the speed of heat propagation of $C = \sqrt{\alpha/\tau}$ in the case of RHE. In order to assess the effect of the different values of τ and C on the differences in the temperature profiles, in Fig. 4 we plotted the percentage differences between the solutions from HHE and FHE, and between RHE and FHE. These differences were higher at the start of heating and for locations close to the electrode surface. The differences were seen to increase for higher values of thermal relaxation time in HHE or equivalently for lower values of the speed of heat propagation in RHE (note the decrease in the maximum percentage difference from 6% to 3% in the case of HHE and from -7% to -4.5% in the case of RHE when τ was reduced from 16 to 8 s.

4 Discussion

The objective of this study was to compare the temperature profiles in biological tissues during RF ablation computed from the Fourier-based, hyperbolic, and relativistic heat conduction models. As far as we know, this is the first time these three models have been compared. The relativistic approach was originally described by Ali and Zhang [12] (2005) as an alternative heat conduction model, since the Fourier heat equation assumes an infinite heat propagation speed, and also because there are grounds for believing that the hyperbolic heat conduction model may violate a more general non-equilibrium second law of thermodynamics. Our study did not try to elucidate which model is true, but to qualitatively describe how each approach works for the mathematical modeling of heating of biological tissue, and especially to identify the differences in the computed temperature profiles. In fact, Ali and Zhang [12] (2005) did not compare the thermal performance of the relativistic model with the others models. In this respect, our results showed that RHE temperature values were always lower than those of the FHE, where in general the computed temperature in the HHE is higher than the FHE, except at the early stages of heating and at points away from the electrode. Note that if there is no heat sources and the temperature at the boundary would be constant, the relativistic solution would coincide with the hyperbolic one taking $C^2 = \alpha/\tau$.

Although most experimentally validated theoretical models consider FHE (Jain and Wolf [24] 2000, Labonte [25] 1994), some studies have suggested that HHE results match experimental results better than FHE when modeling short pulse laser irradiation (Jaunich *et al* [26] 2008). However the temperature peaks predicted by HHE for some specific points and times have not been usually reported in experimental studies, probably because it is difficult that the those peaks are taken in the time and spatial sampling process. Moreover, it could be also difficult to observe those temperature peaks in numerical studies due to the numerical oscillations around of sharp discontinuities. Finally, it is important to note that the RHE temperature profiles did not show these irregularities.

This study has a limitation related to the simplicity of the model geometry. We considered a spherical electrode totally surrounded by infinite and homogenous tissue, with thermal and electrical characteristics constant with temperature. All this allowed a one-dimensional scenario, and hence an analytical solution for the three models studied. However, we should point out that our goal was not to obtain accurate and realistic biological tissue heating models from the three equations (which can be achieved with numerical methods), but to conduct a preliminary assessment of the thermal performance of each thermal model. In spite of the power and accuracy of current numerical methods to realistically model the EBATs, we consider it essential to first use a comparative approach with an analytical solution, as reported here.

Our modeling study did not include the blood perfusion term, which is one of the most important characteristic of the Bioheat Equation. In spite of this, this term acts removing heat such as has been observed in computer simulations [27] and hence implies that the temperatures profiles are lower than in the case without perfusion. Consequently, we think that our comparison among models would not change in presence of the blood

perfusion term.

As regards the most suitable heat model for RFA, in the light of our results future experimental and theoretical studies should be conducted that could consider not only FHE and HHE, but also RHE. The present results also confirm that the non-Fourier heat equations are suitable for modeling temperature for short-time heating close to the heat source, since that the solutions of all the models converged for infinite time or infinite distance from the electrode.

There is still a controversy around the value of thermal relaxation time in biological tissues. Although Mitra *et al.* [13] (1995) measured values around 16 seconds in processed meat, Ali and Zhang's [12] (2005) reported a smaller value. Likewise, Kaminski [7] (1990) reported a relaxation time between 20 s and 30 s for meat products and Vedavarz *et al.* [22] (1994) found an interval between 1 s and 100 s for some biological tissues at room temperature. In this respect, the relativistic heat theory considers a similar parameter C, known as speed of heat propagation, which is somehow inversely proportional to τ. Ali and Zhang [12] (2005) found experimentally that the speed of heat (second sound) is about one order of magnitude less than the speed of sound. If we consider a value of the sound propagation in biological tissues around 1500 m/s, this would imply a value of C around 150 m/s, which for a value of α around 1.5 10^{-7} m^2/s, would estimate τ as α/C^2, i.e. a value around of 6.7 10^{-12}s. In practical terms, this means that the relativistic and hyperbolic heat models would only be useful for very short heating times in biological tissues. However, Ali and Zhang [12] (2005) also point out that these relations are for metals and perfect structures. On the other hand, non-homogeneous materials, such as biological tissues, have very long relaxation times, and consequently would have very low heating speeds (Mitra *et al.* [13] 1995, Kaminski [7] 1990). Unfortunately, no experimental data have been published to date on the speed of heat propagation in biological tissues.

5 Conclusions

Our findings suggest that temperature values obtained from a model with RHE are always lower than those of the FHE, while HHE values are higher than the FHE, except for the initial heating stage and at points away from the electrode. Both HHE and RHE are mathematically hyperbolic, but temperature profile peaks are only observed with HHE. The three solutions converged for infinite time or infinite distance from the electrode. The percentage differences between the FHE and the other solutions are larger for higher values of thermal relaxation time in HHE or equivalently for lower values of the speed of heat propagation in RHE.

A Appendix: Computation of the inverse Laplace transform in the RHE

A.1 Computation of $\mathfrak{L}^{-1}[F_1]$

By the translation theorem for Laplace transforms and formula 36, chapter 5, section 5.6 from Erdélyi *et al* [28] (1954) we have

$$\mathfrak{L}^{-1}\left[\frac{e^{-\sqrt{s+\lambda\,s^2}\,(u-\rho)}}{\sqrt{s+\lambda\,s^2}}\right](\rho,\xi)=\mathfrak{L}^{-1}\left[\frac{e^{-\sqrt{\lambda}\sqrt{\left(s+\frac{1}{2\,\lambda}\right)^2-\frac{1}{4\,\lambda^2}}(u-\rho)}}{\sqrt{\lambda}\sqrt{\left(s+\frac{1}{2\,\lambda}\right)^2-\frac{1}{4\,\lambda^2}}}\right](\rho,\xi)=$$

$$\frac{e^{-\frac{\xi}{2\,\lambda}}}{\sqrt{\lambda}}\,\mathfrak{L}^{-1}\left[\frac{e^{-(u-\rho)\sqrt{\lambda}\sqrt{s^2-\frac{1}{4\,\lambda^2}}}}{\sqrt{s^2-\frac{1}{4\,\lambda^2}}}\right](\rho,\xi)=\frac{e^{-\frac{\xi}{2\,\lambda}}}{\sqrt{\lambda}}\,H\big(\xi-\sqrt{\lambda}(u-\rho)\big)\,I_0\left(\frac{1}{2\,\lambda}\,\sqrt{\xi^2-\lambda(u-\rho)^2}\right)$$

and hence

$$\mathfrak{L}^{-1}\left[\frac{e^{-\sqrt{s+\lambda\,s^2}\,(u-\rho)}}{s\,\sqrt{s+\lambda\,s^2}}\right](\rho,\xi)=\int_0^{\xi}\frac{e^{-\frac{v}{2\,\lambda}}}{\sqrt{\lambda}}\,H\big(v-\sqrt{\lambda}(u-\rho)\big)\,I_0\left(\frac{1}{2\,\lambda}\,\sqrt{v^2-\lambda(u-\rho)^2}\right)\,dv=$$

$$\int_{\sqrt{\lambda}(u-\rho)}^{\xi}\frac{e^{-\frac{v}{2\,\lambda}}}{\sqrt{\lambda}}\,I_0\left(\frac{1}{2\,\lambda}\,\sqrt{v^2-\lambda(u-\rho)^2}\right)\,dv$$

and hence

$$\mathfrak{L}^{-1}[F_1](\rho,\xi)=$$

$$\int_{\rho}^{\infty}\left(\int_0^{\xi}\frac{e^{-\frac{v}{2\lambda}}}{\sqrt{\lambda}}H\big(v-(u-\rho)\sqrt{\lambda}\big)I_0\big(\frac{1}{2\lambda}\sqrt{v^2-\lambda(u-\rho)^2}\big)\,dv\right)\,\frac{du}{u^3}=$$

$$\int_{\rho}^{\infty}H\big(\xi-(u-\rho)\sqrt{\lambda}\big)\left(\int_{(u-\rho)\sqrt{\lambda}}^{\xi}\frac{e^{-\frac{v}{2\lambda}}}{\sqrt{\lambda}}I_0\left(\frac{1}{2\lambda}\sqrt{v^2-\lambda(u-\rho)^2}\right)\,dv\right)\,\frac{du}{u^3}=$$

$$\int_{\rho}^{\rho+\frac{\xi}{\sqrt{\lambda}}}\left(\int_{(u-\rho)\sqrt{\lambda}}^{\xi}\frac{e^{-\frac{v}{2\lambda}}}{\sqrt{\lambda}}I_0\left(\frac{1}{2\lambda}\sqrt{v^2-\lambda(u-\rho)^2}\right)\,dv\right)\,\frac{du}{u^3}\qquad(31)$$

A.2 Computation of $\mathfrak{L}^{-1}[F_2]$

In an analogous way we obtain

$$\mathfrak{L}^{-1}[F_2](\rho,\xi)=$$

$$\int_1^\rho \left(\int_0^\xi \frac{e^{-\frac{v}{2\lambda}}}{\sqrt{\lambda}} H\big(v-(\rho-u)\sqrt{\lambda}\big) I_0\left(\frac{1}{2\lambda}\sqrt{v^2-\lambda(\rho-u)^2}\right)\, dv \right) \frac{du}{u^3} =$$

$$\int_1^\rho \left(H\big(\xi-(\rho-u)\sqrt{\lambda}\big) \int_{(\rho-u)\sqrt{\lambda}}^\xi \frac{e^{-\frac{v}{2\lambda}}}{\sqrt{\lambda}} I_0\left(\frac{1}{2\lambda}\sqrt{v^2-\lambda(\rho-u)^2}\right)\, dv \right) \frac{du}{u^3}$$

Remark that

$$\rho - \frac{\xi}{\sqrt{\lambda}} \geq 1 \quad \text{and} \quad 1 \leq u \leq \rho - \frac{\xi}{\lambda} \Longrightarrow \frac{\xi}{\sqrt{\lambda}} - (\rho - u) \leq 0$$

and

$$\rho - \frac{\xi}{\sqrt{\lambda}} \leq 1 \quad \text{and} \quad 1 \leq u \leq \rho \Longrightarrow \frac{\xi}{\sqrt{\lambda}} - (\rho - u) = u - \left(\rho - \frac{\xi}{\sqrt{\lambda}}\right) \geq u - 1 \geq 0$$

Then

$$\mathfrak{L}^{-1}[F_2](\rho,\xi) =$$

$$= \overline{H}(1-\rho+\frac{\xi}{\sqrt{\lambda}}) \int_1^\rho \left(\int_{(\rho-u)\sqrt{\lambda}}^\xi \frac{e^{-\frac{v}{2\lambda}}}{\sqrt{\lambda}} I_0\left(\frac{1}{2\lambda}\sqrt{v^2-\lambda(\rho-u)^2}\right)\, dv \right) \frac{du}{u^3} +$$

$$H\left(\rho - \frac{\xi}{\sqrt{\lambda}} - 1\right) \int_{\rho-\frac{\xi}{\sqrt{\lambda}}}^\rho \left(\int_{(\rho-u)\sqrt{\lambda}}^\xi \frac{e^{-\frac{v}{2\lambda}}}{\sqrt{\lambda}} I_0(\frac{1}{2\lambda}\sqrt{v^2-\lambda(\rho-u)^2})\, dv \right) \frac{du}{u^3} \qquad (32)$$

where $\overline{H}(x) = 0$ if $x \leq 0$ and $\overline{H}(x) = 1$ if $x > 0$.

A.3 Computation of $\mathfrak{L}^{-1}[F_3]$

Computation of $\mathfrak{L}[F_3](\rho,\xi)$ is more involved. By convolution theorem (convolution is denoted by $*$) we have

$$\mathfrak{L}^{-1}[F_3](\rho,\xi) =$$

$$\int_1^\infty \left(\mathfrak{L}^{-1}\left[\frac{e^{-\sqrt{s+\lambda s^2}(u+\rho-2)}}{s\sqrt{s+\lambda s^2}} \left(1 - \frac{2(1+Bs)}{\sqrt{s+\lambda s^2}+(1+Bs)}\right)\right](\rho,\xi) \right) \frac{du}{u^3} =$$

$$\int_1^\infty \left(\mathfrak{L}^{-1}\left[\frac{e^{-\sqrt{s+\lambda s^2}(u+\rho-2)}}{\sqrt{s+\lambda s^2}} \right](\rho,\xi) * \mathfrak{L}^{-1}\left[\frac{1}{s}\left(1 - \frac{2(1+Bs)}{\sqrt{s+\lambda s^2}+(1+Bs)}\right)\right](\xi) \right) \frac{du}{u^3} \qquad (33)$$

As above we have

$$\mathfrak{L}^{-1}\left[\frac{e^{-\sqrt{s+\lambda s^2}(u+\rho-2)}}{\sqrt{s+\lambda s^2}} \right](\rho,\xi) =$$

$$H\big(\xi-\sqrt{\lambda}(u+\rho-2)\big)\,\frac{e^{-\frac{\xi}{2\lambda}}}{\sqrt{\lambda}}\,I_0\left(\frac{1}{2\lambda}\sqrt{\xi^2-\lambda(u+\rho-2)^2}\right):=$$

$$H\big(\xi-\sqrt{\lambda}(u+\rho-2)\big)\,G_1(\rho,\xi) \tag{34}$$

On the other hand

$$\mathfrak{L}^{-1}\left[\frac{1}{s}\left(1-\frac{2(1+Bs)}{\sqrt{s+\lambda s^2}+(1+Bs)}\right)\right](\xi)=1-\mathfrak{L}^{-1}\left[\frac{2(1+Bs)}{s\big(\sqrt{s+\lambda s^2}+(1+Bs)\big)}\right](\xi)=$$

$$1-\mathfrak{L}^{-1}\left[\left(2B+\frac{2}{s}\right)\frac{1}{\sqrt{s+\lambda s^2}+(1+Bs)}\right](\xi)=$$

$$1-2B\;\mathfrak{L}^{-1}\left[\frac{1}{\sqrt{s+\lambda s^2}+(1+Bs)}\right](\xi)-2\;\mathfrak{L}^{-1}\left[\frac{1}{s\big(\sqrt{s+\lambda s^2}+(1+Bs)\big)}\right](\xi)$$

The last inverse can be computed with help of a Bromwich's contour. There are two branch points $s=0$ and $s=-\frac{1}{\lambda}$ and two possible poles verifying

$$1+(2\;B-1)\;s+(B^2-\lambda)\;s^2=0\quad\Longrightarrow\quad s=\frac{-(2\;B-1)\pm\sqrt{1+4\;\lambda-4\;B}}{2\;(B^2-\lambda)}$$

Put

$$s_1=\frac{-(2\;B-1)+\sqrt{1+4\;\lambda-4\;B}}{2\;(B^2-\lambda)},\qquad s_2=\frac{-(2\;B-1)-\sqrt{1+4\;\lambda-4\;B}}{2\;(B^2-\lambda)}$$

In our case $s_1<-\frac{1}{\lambda},\ s_2<-\frac{1}{\lambda}$, $1+B\;s_1>0$ and $1+B\;s_2<0$. Then only s_1 is a pole. Using that $\sqrt{s_1+\lambda\;s_1^2}=-(1+B\;s_1)$ and L'Hôpital's rule, the residue is

$$Res[f;s_1]=\lim_{s\to s_1}\frac{(s-s_1)e^{s\xi}}{s\big(\sqrt{s+\lambda\;s^2}+1+B\;s\big)}=\frac{e^{s_1\;\xi}}{s_1}\lim_{s\to s_1}\frac{1}{\frac{1+2\;\lambda\;s}{2\sqrt{s+\lambda\;s^2}}+B}=$$

$$-\frac{e^{s_1\;\xi}}{s_1}\frac{2(1+B\;s_1)}{1-2\;B+(2\;\lambda-2\;B^2)\;s_1}$$

Then

$$\mathfrak{L}^{-1}\left[\frac{1}{s\big(\sqrt{s+\lambda s^2}+(1+Bs)\big)}\right](\xi)=$$

$$1+Res[f;s_1]+\frac{1}{\pi}\int_0^{\frac{1}{\lambda}}\frac{\sqrt{s-\lambda s^2}\;e^{-s\;\xi}}{s\big(-1-(1-2\;B)\;s+(\lambda-B^2)\;s^2\big)}\;ds$$

Now we have

$$\mathfrak{L}^{-1}\left[\frac{1}{\sqrt{s+\lambda\ s^2}+1+B\ s}\right](\xi)=\frac{d}{d\,\xi}\mathfrak{L}^{-1}\left[\frac{1}{s\big(\sqrt{s+\lambda\ s^2}+1+B\ s\big)}\right](\xi)=$$

$$-2\ \frac{e^{\xi\ s_1}(1+B\ s_1)}{1-2\ B+(2\ \lambda-2\ B^2)\ s_1}-\frac{1}{\pi}\int_0^{\frac{1}{\lambda}}\frac{\sqrt{s-\lambda s^2}\ e^{-s\,\xi}}{-1-(1-2\ B)\ s+(\lambda-B^2)\ s^2}\ ds$$

We obtain

$$G_2(\xi):=\mathfrak{L}^{-1}\left[\frac{1}{s}\left(1-\frac{2(1+Bs)}{\sqrt{s+\lambda s^2}+(1+Bs)}\right)\right](\xi)=$$

$$-1+\left(B+\frac{1}{s_1}\right)\frac{4\ e^{\xi\ s_1}(1+B\ s_1)}{1-2\ B+(2\ \lambda-2\ B^2)\ s_1}$$

$$+\frac{2}{\pi}\int_0^{\frac{1}{\lambda}}\left(B-\frac{1}{s}\right)\frac{\sqrt{s-\lambda s^2}\ e^{-s\,\xi}}{-1-(1-2\ B)\ s+(\lambda-B^2)\ s^2}\ ds \tag{35}$$

Then by (33), (A.3) and (35) we have

$$\mathfrak{L}^{-1}[F_3](\rho,\xi)=\int_1^\infty\left(\int_0^\xi G_1(\rho,w)\ G_2(\xi-w)\ dw\right)\ \frac{du}{u^3}=$$

$$\int_1^\infty H\big(\xi-\sqrt{\lambda}(u+\rho-2)\big)\left(\int_{\sqrt{\lambda}(u+\rho-2)}^\xi G_1(\rho,w)G_2(\xi-w)\ dw\right)\ \frac{du}{u^3}=$$

$$H\left(\frac{\xi}{\sqrt{\lambda}}-\rho+1\right)\int_1^{\frac{\xi}{\sqrt{\lambda}}-\rho+2}\left(\int_{\sqrt{\lambda}(u+\rho-2)}^\xi G_1(\rho,w)G_2(\xi-w)\ dw\right)\ \frac{du}{u^3} \tag{36}$$

Financial support

This work received financial support from the Spanish Government (Ministerio de Ciencia e Innovación, Ref. TEC2011-27133-C02-01).

References

[1] Wazni O., Wilkoff, B. and Saliba, W. 2011 Catheter ablation for atrial fibrillation *N. Engl. J. Med.* **365**, (24), 2296-2304.

[2] Salas, N., Castle, S. M. and Leveillee, R. J. 2011 Radiofrequency ablation for treatment of renal tumors: technological principles and outcomes. *Expert Rev. Med. Devices* **8**, (6), 695-707.

[3] Berjano, E. J. 2006 Theoretical modeling for radiofrequency ablation: state-of-the-art and challenges for the future. *Biomed. Eng. Online* 5-24

[4] Pennes, H. H. 1948 Analysis of tissue and arterial blood temperatures in the resting human forearm. *J. Appl. Physiol.* **1**, 93-122.

[5] Liu, J., Chen, X. and Xu, L. X. 1999 New thermal wave aspects on burn evaluation of skin subjected to instantaneous heating. *IEEE Trans. Biomed. Eng.* **46**, 420-428.

[6] Shih, T. C., Kou, H. S., Liauh, C. T. and Lin, W. L. 2005 The impact of thermal wave characteristics on thermal dose distribution during thermal therapy: a numerical study. *Med. Phys.* **32** 3029-3036.

[7] Kaminski, W. 1990 Hyperbolic heat conduction for materials with a nonhomogeneous inner structure. *ASME J. Heat Transfer* **112**, (3), 555-560.

[8] Zhang, D. M., Li, L., Li, Z. H., Guan, L., Tan, X. and Liu, D. 2006 Non-Fourier heat conduction studying on high-power short-pulse laser ablation considering heat source effect. *Eur. Phys. J. Appl. Phys.* **33** 91-96.

[9] Morse, P. M. and Feshbach, H. 1953 *Methods of Theoretical Physics*. New York: McGraw-Hill.

[10] Tisza, L. 1938 *C. R. Acad. Sci.* **207**, 1035 and **207** 1186.

[11] Landau, L. D. 1941 *J. Phys. USSR* **5**, 71.

[12] Ali, Y. M. and Zhang, L. M. 2005 Relativistic heat conduction. *Int. J. Heat Mass Transfer* **48**, 2397-2406.

[13] Mitra, K., Kumar, S., Vedavarz, S. and Moallemi, M. K. 1995 Experimental evidence of hyperbolic heat conduction in processed meat. *ASME J. Heat Transfer* **117**, 568-573.

[14] Cattaneo, C. R. 1958 Sur une forme de l'équation de la chaleur éliminant le paradoxe d'une propagation instantanée. *Comptes Rendus* **247**, (4), 431-433.

[15] Vernotte, P. 1958 Les paradoxes de la theorie continue de l'équation de la chaleur. *Comptes Rendus* **246**, (22), 3154-3155.

[16] Tzou, D. Y. 1992 Thermal shock phenomena under high-rate response in solids. In *Chang-Lin Tine (Ed.), Annual Review of Heat Transfer*, Chap. 3, pp. 111-85. Washington D. C.: Hemisphere Publishing Inc.

[17] Özişik, M. N. and Tzou, D. Y. 1994 On wave theory in heat conduction. *ASME J. Heat Tranfer* **116**, 526-535.

[18] Barletta, A. and Zanchini, E. 1997 Hyperbolic heat conduction and local equilibrium: a second law analysis. *Int. J. Heat Mass Transfer* **40**, (5), 1007-1016.

[19] López Molina, J. A., Rivera, M. J., Trujillo, M. and Berjano, E. J. 2008 Effect of the thermal wave in radiofrequency ablation modeling: an analytical study. *Phys. Med. Biol.* **53**, (5), 1447-1462.

[20] Kim, K. and Guo, Z. 2007 Multi-time-scale heat transfer modeling of turbid tissues exposed to short-pulsed irradiations. *Computer Methods and Programs in Biomedicine* **86**, 112-123.

[21] Erez, A. and Shitzer, A. 1980 Controlled destruction and temperature distributions in biological tissues subjected to monoactive electroagulation. *J. Biomech. Eng.* **102**, 42-49.

[22] Vedavarz, A., Kumar, S. and Moalleni, M. K. 1994 Significance of non-Fourier heat waves in conduction. *J. Heat Transfer, Trans, ASME* **116**, 221-224.

[23] Watson, G. N. 1995 *A treatise on the theory of Bessel functions* Cambridge: Cambridge University Press

[24] Jain, M. K. and Wolf, P. D. 2000 A three-dimensional finite element model of radiofrequency ablation with blood flow and its experimental validation. *Ann. Biomed. Eng.* **28**, 1075-1084.

[25] Labonte, S. 1994 Numerical model for radio-frequency ablation of the endocardium and its experimental validation. *IEEE Trans. Biomed. Eng.* **41**, 108-115.

[26] Jaunich, M., Raje, S., Kim, K., Mitra, K. and Guo, Z. 2008 Bio-heat transfer analysis during short pulse laser irradiation of tissues. *Int. J. Heat Mass Transfer* **51**, 5511-5521.

[27] Chang, I. 2003 Finite element analysis of hepatic radiofrequency ablation probes using temperature-dependent electrical conductivity. *Biomed Eng Online.* May 8;2:12.

[28] Erdélyi, A., Magnus, W., Oberhettinger, M. F. and Tricomi, F. G. 1954 *Tables of integral transforms I.* New York: McGraw-Hill.

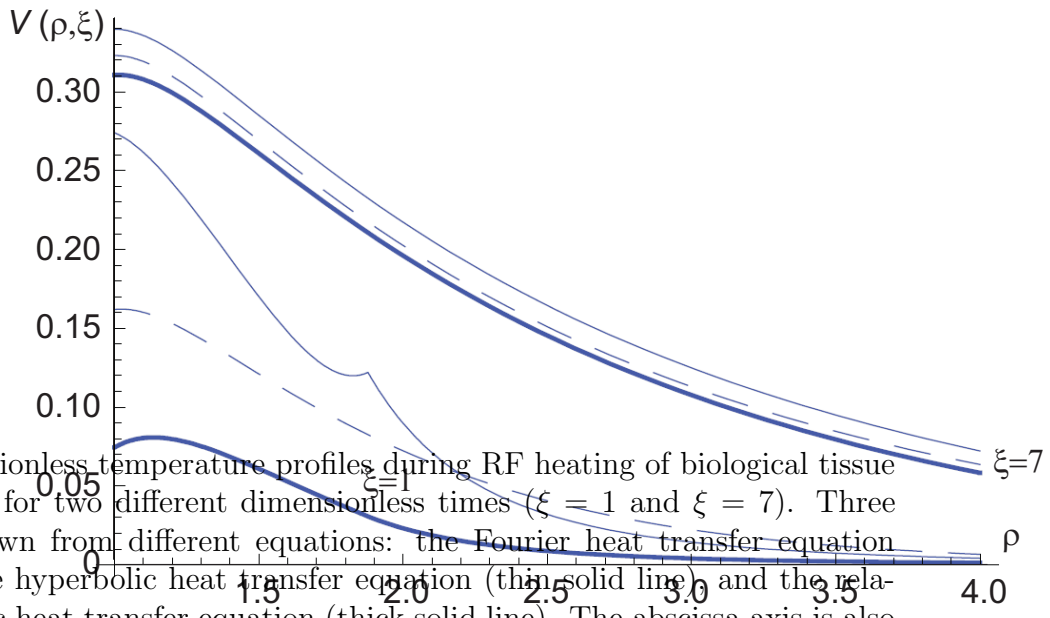

Figure 1: Dimensionless temperature profiles during RF heating of biological tissue along radial axis for two different dimensionless times ($\xi = 1$ and $\xi = 7$). Three solutions are shown from different equations: the Fourier heat transfer equation (dashed line), the hyperbolic heat transfer equation (thin solid line), and the relativistic hyperbolic heat transfer equation (thick solid line). The abscissa axis is also normalized to the electrode radius r_0 (i.e. dimensionless distance is r/r_0). Dimensionless thermal relaxation time of the biological tissue was $\lambda = 1.2963$ (equivalent to $\tau = 16\ s$).

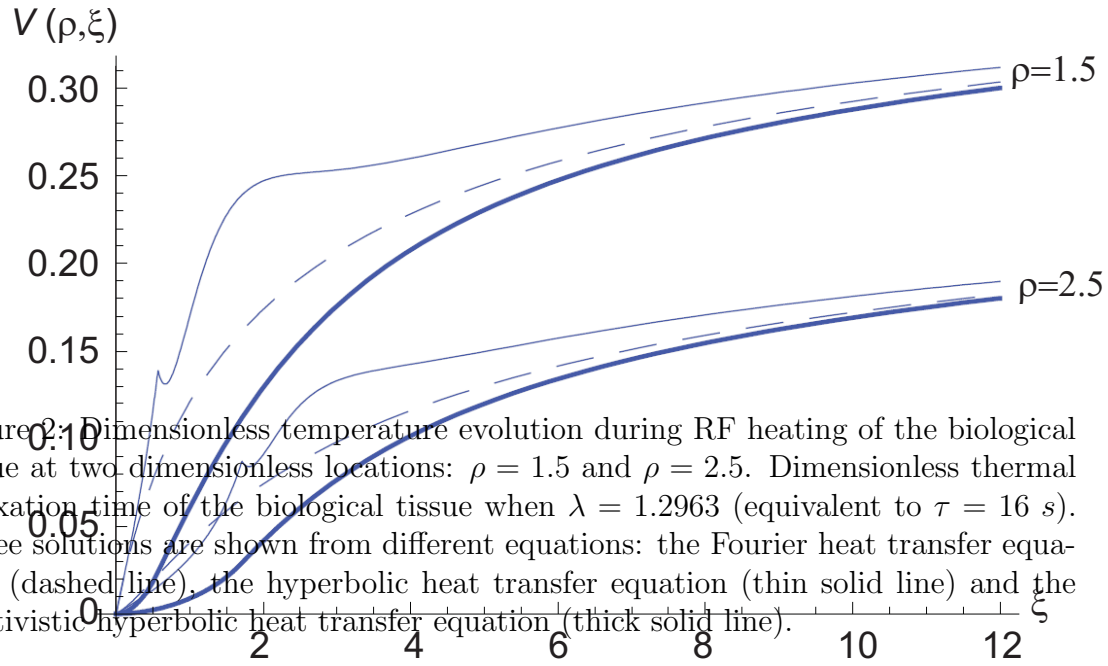

Figure 2: Dimensionless temperature evolution during RF heating of the biological tissue at two dimensionless locations: $\rho = 1.5$ and $\rho = 2.5$. Dimensionless thermal relaxation time of the biological tissue when $\lambda = 1.2963$ (equivalent to $\tau = 16\ s$). Three solutions are shown from different equations: the Fourier heat transfer equation (dashed line), the hyperbolic heat transfer equation (thin solid line) and the relativistic hyperbolic heat transfer equation (thick solid line).

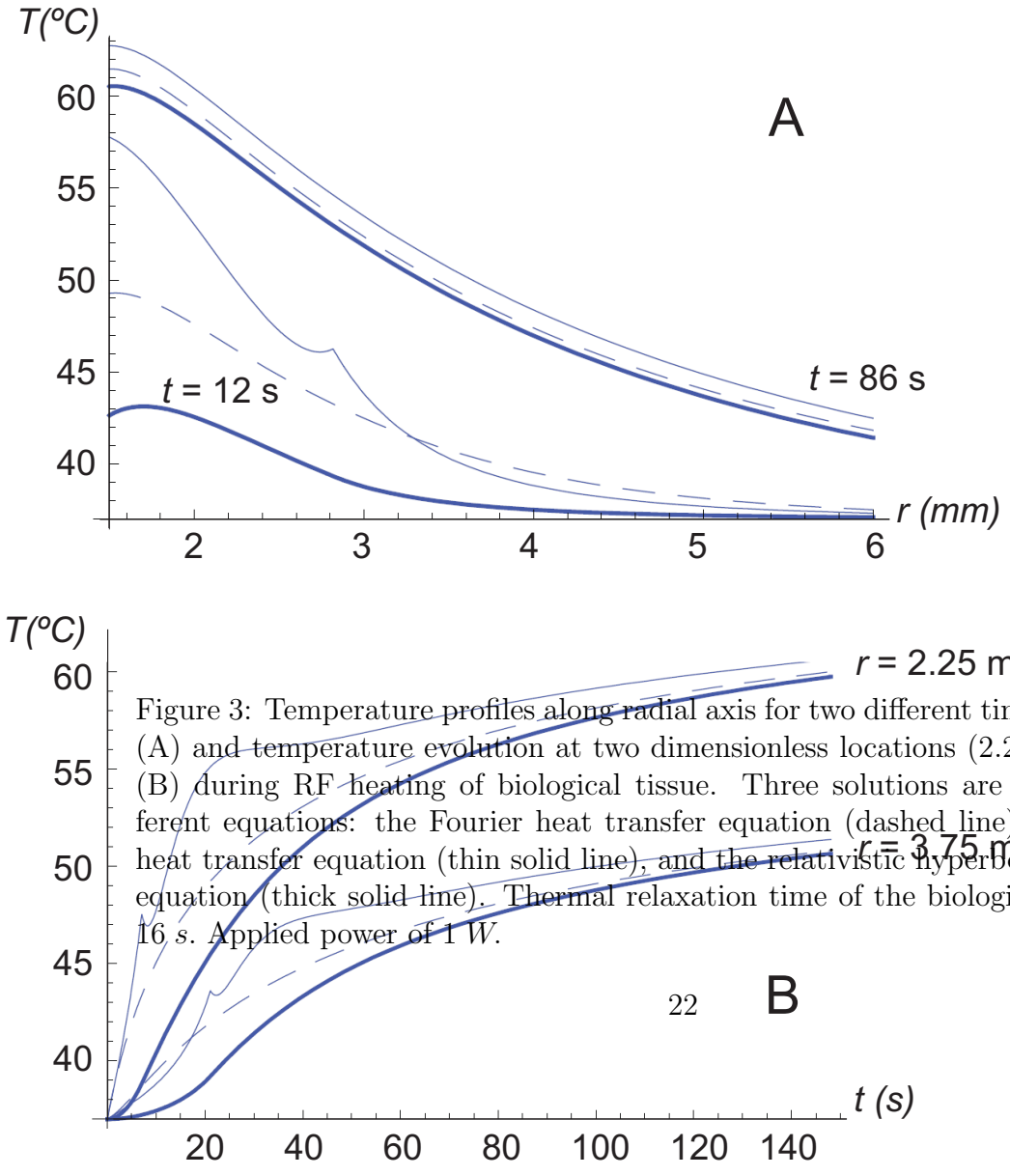

Figure 3: Temperature profiles along radial axis for two different times (12 and 86 s) (A) and temperature evolution at two dimensionless locations (2.25 and 3.75 mm) (B) during RF heating of biological tissue. Three solutions are shown from different equations: the Fourier heat transfer equation (dashed line), the hyperbolic heat transfer equation (thin solid line), and the relativistic hyperbolic heat transfer equation (thick solid line). Thermal relaxation time of the biological tissue was of 16 s. Applied power of 1 W.

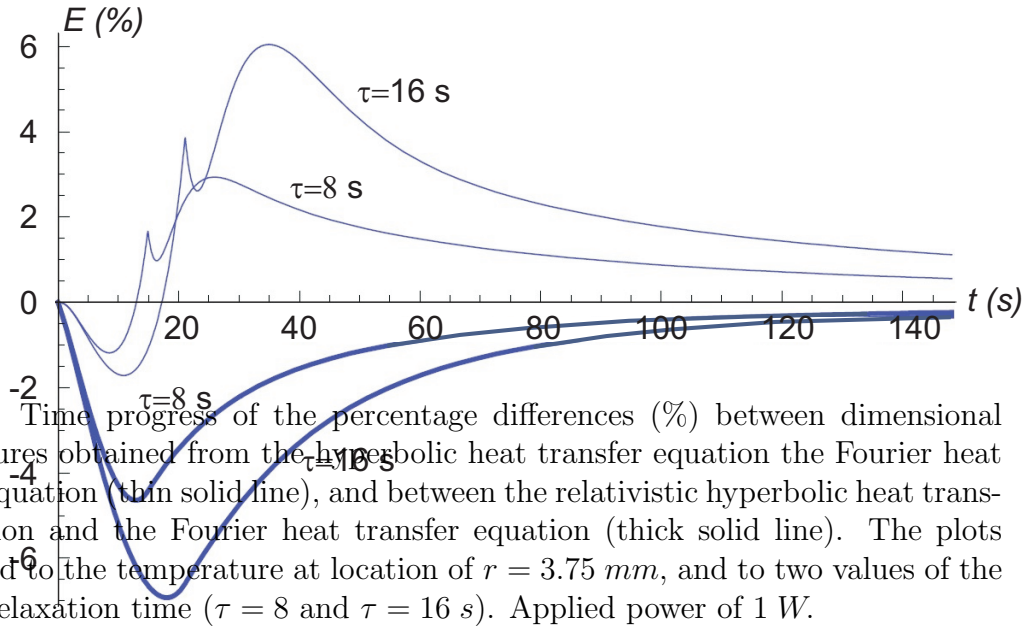

Figure 4: Time progress of the percentage differences (%) between dimensional temperatures obtained from the hyperbolic heat transfer equation the Fourier heat transfer equation (thin solid line), and between the relativistic hyperbolic heat transfer equation and the Fourier heat transfer equation (thick solid line). The plots correspond to the temperature at location of $r = 3.75\ mm$, and to two values of the thermal relaxation time ($\tau = 8$ and $\tau = 16\ s$). Applied power of 1 W.